

# Towards a microscopic description of the fission process

*H. Goutte, N. Dubray, and J.-F. Berger*  
CEA, DAM, DIF, F-91297 Arpajon, France

## **Abstract**

One major issue in nuclear physics is to develop a consistent model able to describe on the same footing the different aspects of the fission process, i.e. properties of the fissioning system, fission dynamics and fragment distributions. Microscopic fission studies based on the mean-field approximation are here presented.

## **1 Motivations**

Many theoretical studies of the fission process have been undertaken these last years all over the world. These works are mainly motivated by:

- Fundamental questions: fission is a process, which is not fully understood yet. From a theoretical point of view, fission appears as a large amplitude motion, in which intervene i) configurations far from equilibrium, a large rearrangement of the internal structure of the nucleus with an important role played by the shell effects, ii) many types of deformations simultaneously, and iii) dynamical effects such as the couplings between different collective modes, and/or the couplings between collective modes and intrinsic excitations. Some open questions remain: what about the role played by shell effects  $A=132$  and/or  $A=140$  as a function of the fissioning system, and excitation energy? What about dissipation, friction? What are the collective modes pertinent during the process?
- A large amount of new experimental results: fission is now studied in new conditions. Data are now obtained for exotic nuclei, super heavies, for new energy ranges ...
- The need for predictions for nuclear data both for energy production and production of exotic nuclei (for instance ALTO, Orsay France and SPIRAL2, Caen France).
- New super-calculators: The new computing powers make possible to develop new approaches and to perform large scale calculations.

In Bruyères-le-Châtel fission studies have restart these last years in order to have a description:

- as “ab-initio” as possible,
- applicable to the different aspects of the process,
- able to give quantitative results, which can be directly compared to experimental data.

The ultimate goal would be to have a coherent description of the structure of the fissioning nucleus, of the fission fragments, and of the dynamics of the process.

## 2 Formalism

Different approaches are under development in the community (for instance “mean-field instanton” by J. Skalski [1]). In Bruyères-le-Châtel we have developed a microscopic time dependent quantum mechanical approach of the fission process, based on the Time Dependent Generator Coordinate Method (TD-GCM) with the Gaussian Overlap Approximation (GOA), where basis states are obtained from constrained Hartree-Fock-Bogoliubov (HFB) calculations using the Gogny D1S force [2][3].

In the present work we assume that:

- Fission dynamics is governed by the evolution of only two collective coordinates, namely the axial quadrupole  $q_{20}$  and octupole  $q_{30}$  moments.

- The internal structure is at equilibrium at each step of the collective motion. (We assume that the characteristic time for the collective motion is much longer than the time for the intrinsic motion. Then, collective and intrinsic degrees of freedom are treated separately.)

- The evolution is adiabatic (only the lowest intrinsic state is populated at each step of the collective motion. In other words, single-particle excitations are not taken into account.)

- Once a scission configuration is reached, splitting of the nucleus will occur irremediably, yielding two separated fragments moving away from each other under the action of their mutual Coulomb repulsion. Observable fragment properties can be inferred from the characteristics of the nascent fragments at scission.

With these assumptions, fission dynamics results from a time evolution in a two-dimensional collective space

$$|\Psi(t)\rangle = \int dq_{20} dq_{30} f(q_{20}, q_{30}, t) |\Phi_{q_{20}q_{30}}\rangle. \quad (1)$$

The basis states  $|\Phi_{q_{20}q_{30}}\rangle$  are determined from constrained Hartree-Fock-Bogoliubov calculations based on the minimization principle:

$$\delta \left\langle \Phi_{q_{20}q_{30}} \left| \hat{H} - \sum_i \lambda_i \hat{Q}_{i0} - \lambda_N \hat{N} - \lambda_Z \hat{Z} \right| \Phi_{q_{20}q_{30}} \right\rangle = 0, \quad (2)$$

where the Lagrange parameters are determined from

$$\begin{cases} \left\langle \Phi_{q_{20}q_{30}} \left| \hat{N}(\hat{Z}) \right| \Phi_{q_{20}q_{30}} \right\rangle = N(Z) \\ \left\langle \Phi_{q_{20}q_{30}} \left| \hat{Q}_{i0} \right| \Phi_{q_{20}q_{30}} \right\rangle = q_{i0}. \end{cases} \quad (3)$$

In Eq. (2)  $Q_{i0}$  is the set of external operators,  $Q_{20}$ ,  $Q_{30}$  and  $Q_{10}$ , and  $H$  is the nuclear many-body effective Hamiltonian built with the effective D1S Gogny force. The constraint on the isoscalar dipole mass operator is introduced to fix the position of the center of mass of the whole system.

The Bogoliubov space has been restricted by enforcing axial symmetry along the  $z$  axis and the self consistent  $\Pi_2$  symmetry where  $T$  is the time reversal operator and  $\Pi_2$  the reflection with respect

to the xOz plane. Let us note that symmetry-unrestricted DFT calculations have been performed recently in heavy actinides by A. Staszczak *et al.* [4].

Here, the system of HFB equations has been solved numerically for each set of deformations by expanding the quasi-particle states onto a one-center axial harmonic oscillator basis at small elongation and onto two-center bases for large elongations.

The time-dependent weight functions  $f(q_{20}, q_{30}, t)$  in Eq. (1) are determined from:

$$\frac{\partial}{\partial f^*(q_{20}, q_{30}, t)} \int_{t_1}^{t_2} \langle \psi(t) | \hat{H} - ih \frac{\partial}{\partial t} | \psi(t) \rangle dt = 0, \quad (4)$$

where  $H$  is the same nuclear Hamiltonian as the one introduced in the HFB equations (Eq.(2)). The result is the Hill-Wheeler equation which reduces to a time-dependent Schrodinger equation when the Generator Coordinate Method is solved using the Gaussian Overlap Approximation, namely

$$H_{\text{coll}} g(q_{20}, q_{30}, t) = ih \frac{\partial g(q_{20}, q_{30}, t)}{\partial t}, \quad (5)$$

where  $g$  the collective wave function is the Gauss transform of  $f(q_{20}, q_{30}, t)$  of Eq. (1). The collective Hamiltonian is:

$$H_{\text{coll}} = - \frac{\hbar^2}{2} \sum_{i,j} \frac{\partial}{\partial q_i} B_{ij}(q_{20}, q_{30}) \frac{\partial}{\partial q_j} + \langle \Phi_{q_{20}q_{30}} | \hat{H} | \Phi_{q_{20}q_{30}} \rangle - \Delta V(q_{20}, q_{30}), \quad (6)$$

where  $B_{ij}(q_{20}, q_{30})$  is the inverse of the inertia tensor, and  $\Delta V(q_{20}, q_{30})$  is the sum of the rotational and vibrational zero point energy corrections. Let us note that inertia are here calculated from the adiabatic time-dependent Hartree-Fock theory with the Inglis-Belyaev approximation

### 3 Results

#### 3.1 Potential energy surfaces

Potential energy surfaces are plotted on Fig.1 for  $^{256}\text{Fm}$  and  $^{226}\text{Th}$  isotopes. The most striking feature is that the Potential Energy Surfaces display contrasted topologies. For instance, a minimum is taking place at superdeformation in  $^{226}\text{Th}$ , whereas this minimum does not exist in the Fermium isotope. As previously discussed in Ref. [4], where fission barriers have been calculated for 55 even-even actinides from  $^{226}\text{Th}$  to  $^{262}\text{No}$ , the vanishing of the superdeformed minimum is a common feature of all actinides with a neutron number  $N > 156$ . A third minimum is also predicted in the asymmetric valley ( $q_{30} = 20 \text{ b}^{3/2}$ ) at large elongation ( $q_{20} = 140 \text{ b}$ ) only in  $^{226}\text{Th}$ .

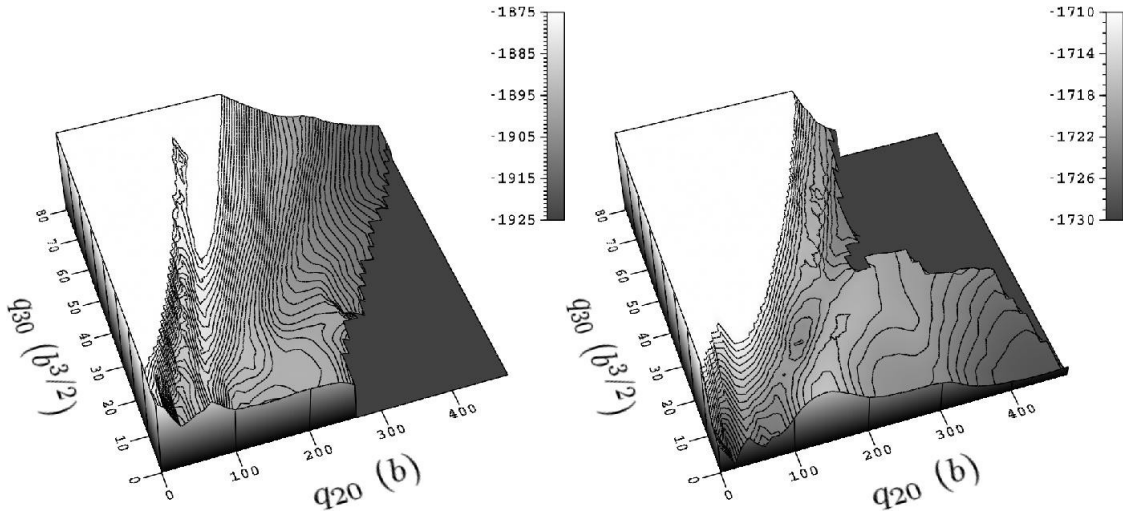


**Fig. 1.** Potential energies (in MeV) as functions of the  $q_{20}$  (b) and  $q_{30}$  ( $b^{3/2}$ ) mass moments for  $^{256}\text{Fm}$  (left panel) and  $^{226}\text{Th}$  (right panel). Post scission points are not plotted.

### 3.2 Shape isomers

Time-independent beyond mean-field calculations have also been performed by use of a five-dimensional collective Hamiltonian (5DCH) derived from the Generator Coordinate Method with the Gaussian Overlap Approximation for the five quadrupole coordinates, that is for axial  $q_{20}$  and triaxial  $q_{22}$  quadrupole deformations and the three rotation degrees of freedom [5]. Shape isomers have been obtained for 55 even-even actinides [6]. Results are shown in Fig. 2, where the excitation energy of the shape isomers is expressed with respect to normal deformed lowest energy states. A good agreement between predictions (dots) and experimental data (open symbols) is found in Thorium, Uranium, Plutonium, and Curium isotopes. A global lowering of isomer energies is predicted as the mass number increases. Superdeformed states are even found to be lower in energy than normal deformed states in  $^{242,244}\text{Fm}$  and  $^{250}\text{No}$ . However, as these states are only a few hundred keV below the octupole unstable outer barrier, they may not survive as bound states.

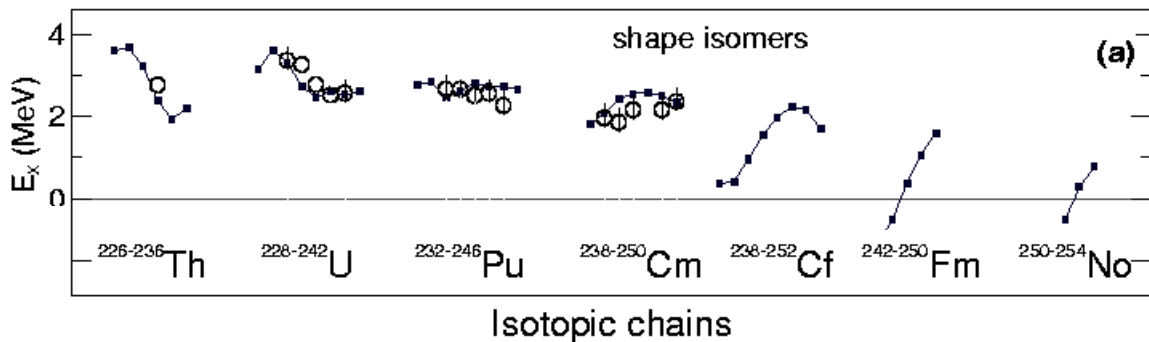


**Fig. 2.** Excitation energy (in MeV) of the shape isomers above respective normal deformed ground states for even-even actinides.

When comparing the  $\gamma$ -back and fission lifetime values that we have obtained from WKB calculations [6], we find that

- shape isomers in Th and U isotopes predominantly decay through  $\gamma$  emission,
- fission and  $\gamma$ -back decays are competing for Pu and Cm elements,
- and finally, fission is by far dominating the decay processes for higher Z elements.

These overall predictions are in qualitative agreement with experimental data available in a few Uranium, Plutonium and Curium isotopes..

### 3.3 Fission fragment properties

Fission fragment properties have been calculated recently for low-energy fission of different actinides using constrained Hartree-Fock-Bogoliubov calculations with a finite-range effective interaction ([7],[8],[9]). Scission configurations are first determined and deformation energy, energy partitioning between the two fragments, prompt fission neutron multiplicities, deviations from unchanged charge distributions, and total kinetic energies are then derived through simple models.

The axial mass quadrupole deformation of the fragments is plotted on Fig. 3 as a function of fragment mass. We clearly see that the curves have a saw-tooth structure with minima for  $A \sim 86$  and  $130$  and maxima for  $\sim 112$  and  $170$ . Indeed, strong spherical shell effects for  $N = 82$  and  $Z = 50$  stabilize spherical fragment of Tin isotopes at scission.

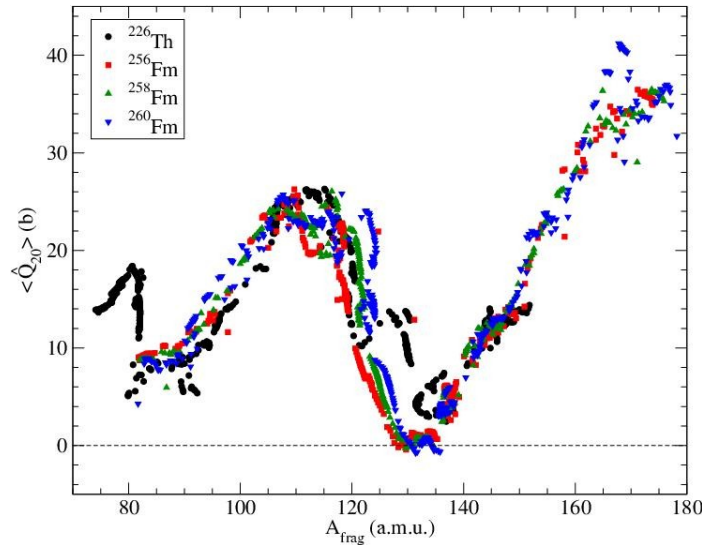


**Fig. 3.** Axial mass quadrupole moments of the nascent fission fragments for  $^{226}\text{Th}$  (squares),  $^{256}\text{Fm}$  (stars),  $^{258}\text{Fm}$  (triangles), and  $^{260}\text{Fm}$  (crosses) as functions of fragment mass.

Prompt neutron emission multiplicity is estimated from the formula

$$\nu(A_{frag}) = \frac{E^*(A_{frag})}{[E_k + B_n^*(A_{frag})]}^{-1}, \quad (7)$$

where  $B_n^*(A_{frag})$  is the one-neutron binding energy of the fragment at scission and where  $E_k$  is the mean neutron energy. In ref.[8], we have assumed that i) there is no intrinsic excitation (the excitation

energy  $E^*(A_{\text{frag}})$  is only deformation energy  $E_{\text{def}}(A_{\text{frag}})$ , and ii) fragments de-excite only through prompt neutron emission with no  $\gamma$  emission.

The fragment deformation energy is derived through

$$E_{\text{def}}(A_{\text{frag}}) = E_{\text{ff}}(A_{\text{frag}}) - E_{\text{gs}}(A_{\text{frag}}), \quad (8)$$

where  $E_{\text{gs}}(A_{\text{frag}})$  is the fragment ground state energy and  $E_{\text{ff}}(A_{\text{frag}})$  is the energy of the nascent fission fragment.  $E_{\text{ff}}(A_{\text{frag}})$  is here calculated from constrained HFB calculations where axial quadrupole and octupole moments are those deduced above at scission configurations (see Fig. 3).

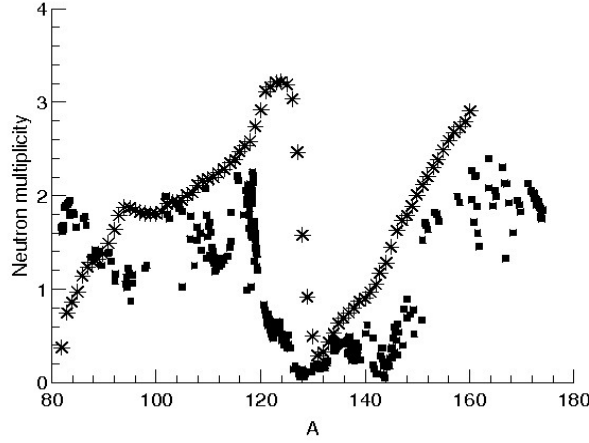


**Fig.4:** Neutron multiplicity for  $^{256}\text{Fm}$ . Comparison between theoretical calculations (squares) and experimental data (stars).

Neutron emission multiplicities are plotted on Fig.4 for  $^{256}\text{Fm}$ . We clearly see that the general trend is well reproduced by our calculations. However, the calculated number of emitted neutrons seems to be globally smaller than the experimental one. This global underestimation is probably due to the neglect in our approach of intrinsic excitations coming from dissipation prior to scission, or to non-fully appropriate criteria to define scission configuration. Along this line, new developments have been undertaken by W. Younes et al. [9] to define a new quantitative criterion to identify scission configurations based on building up a sufficient amount of available energy in the fissioning system to overcome the attractive part of the interaction between fragments.

## 4 Perspectives

We have presented here some studies of low-energy fission of typical actinides such as Fm, Th, Pu and U. However, many other microscopic fission studies are performed in the community such as:

- Fission barriers and potential energy surfaces in heavy, very heavy, and super heavy nuclei. For instance, in [4] symmetry-unrestricted nuclear density functional calculations based on the SkM\* parametrization predict a new phenomenon of trimodal spontaneous fission for some rutherfordium, seaborgium, and hassium isotopes.
- Fission barrier in light nuclei. In [10], fission barriers have been calculated in the light  $^{70}\text{Se}$  nucleus. The  $^{70}\text{Se}$  nucleus having a fissility parameter equals to 0.33, is located below the Businaro-Gallone value, and only conditional fission barriers exist for given fragmentations. The obtained fission barriers for  $^{39}\text{K}+^{31}\text{P}$  and  $^{58}\text{Ni}+^{12}\text{C}$  are compared with the experimental data and are found to overestimate the available data by about 10 MeV.
- Cluster emission: In [11], cluster radioactivity of thorium isotopes is described as a very mass symmetric fission process. One dimensional HFB calculations have been performed with a constraint on the octupole moment. The purpose of the study is to show that cluster radioactivity can be fully described microscopically with the Gogny interaction in the usual framework used to describe fission.
- Angular momentum of the fission fragments at scission: In [12], results of Skyrme-Hartree-Fock plus BCS-pairing calculations of fragment deformabilities are used to deduce a distribution of fission-fragment spins as a function of the fragment total excitation energy. A fairly good agreement is found in the calculated deformed fragments.

This non-exhaustive list strengthen our idea that approaches based on the mean-field are pertinent for a large variety of fission studies, from fission of light nuclei up to superheavies, for symmetric to very asymmetric fragmentations.

## References

- [1] J. Skalsi, *Phys. Rev. C* 77 064610 (2008).
- [2] J. Dechargé and D. Gogny, *Phys. Rev. C* 21 1568 (1980).
- [3] J. F. Berger, M. Girod, and D. Gogny, *Comp. Phys. Comm.* 63 365 (1991).
- [4] A. Staszczak, A. Baran, J. Dobaczewski, and W. Nazarewicz, arxiv: 0906.42481v1 [nucl-th]
- [5] J. Libert, M. Girod, and J.-P. Delaroche, *Phys. Rev. C* 60, 054301 (1999).
- [6] J.P. Delaroche, M. Girod, H. Goutte, and J. Libert., *Nucl. Phys. A* 771 103 (2006).
- [7] H. Goutte, P. Casoli, J.-F. Berger, and D. Gogny, *Phys. Rev. C* 71 024316 (2005).
- [8] N. Dubray, H. Goutte, and J.-P. Delaroche, *Phys. Rev. C* 77 014310 (2008).
- [9] W. Younes, and D. Gogny, to be published in Proc.Fourth Intern.Workshop on Nuclear Fission and Fission-Product Spectroscopy, Cadarache, France, May 13 - 16 2009, A. Chatillon, H.Faust, G.Fioni, D.Goutte, H.Goutte
- [10] L. Bonneau, and P. Quentin, *Phys. Rev. C* 72, 014311 (2005).

- [11] L. M. Robledo, and J. L. Egido, Proc.Third Intern.Workshop on Nuclear Fission and Fission- Product Spectroscopy, Cadarache, France, 11-14 May 2005, H.Goutte, H.Faust, G.Fioni, D.Goutte, Eds., p. 103 (2005); AIP Conf.Proc. 798 (2005)
- [12] L. Bonneau et al., *Phys. Rev. C* 75, 064313 (2007) .